Available online at www.sciencedirect.com

SciVerse ScienceDirect

Procedia Engineering 58 (2013) 77 – 87

Procedia Engineering

www.elsevier.com/locate/procedia

The 12th Hypervelocity Impact Symposium

# Development of a Linear Implosion-Driven Hypervelocity Launcher

Jason Loiseau[a]*, Justin Huneault[a], Andrew J. Higgins[a]

[a]McGill University, 815 Sherbrook Street West, Montreal, H3A OC3, Canada

**Abstract**

A traditional difficulty with high-explosive hypervelocity launching techniques is that extreme loading generally causes hydrodynamic deformation of the projectile either incidentally or by design. The launcher presented in this study uses explosives to operate the pump tube of a two-stage light gas gun via continuous linear implosion. In this configuration, the projectile is cushioned from direct action of the explosives by a light driver gas. The launch cycle is therefore comparable to a conventional two-stage light gas gun but with the shock driven by the rapid linear implosion of the pump tube compressing the gas to a much higher enthalpy. A laboratory scale version of the implosion driven launcher has recently demonstrated the ability to launch a 0.7 g projectile to 7.9 km/s. This design has successfully been scaled up to launch a 15 g projectile to 7.6 km/s, a result comparable to large two-stage light gas guns. This study presents the experimental and computational work performed in the ongoing development of this device. The extreme launch conditions lead to a number of unique design considerations, including dynamic confinment of the driver and launcher reservoir, mitigation of the loss of driver gas, and in-bore projectile stability and survivability. These issues are addressed experimentally through a number of focused launcher trials, as well as through the development of a quasi-one-dimensional Lagrangian hydrocode. The development of advanced implementations that involve continuing explosives onto the reservoir and launch tube in order to maintain a high driving pressure are also considered. These "second stage" techniques offer the potential for achieving projectile velocities in excess of 10 km/s.



*Keywords*: Explosive-Driven Hypervelocity Launcher, Implosion, Light Gas Gun

## 1. Introduction

Despite decades of development, the performance of light gas guns employing purely gasdynamic launch cycles has reached a plateau below the envelope of muzzle velocity, projectile mass, and projectile geometry desirable for orbital debris impact simulation and fundamental equation of state studies. Exceeding the current gas gun performance envelope using only gasdynamic stages is expected to cause irreversible damage to at least part of the gun [1, 2]. With the inevitability of launcher damage in this terminal velocity regime it becomes attractive to use disposable launchers and harness the very large energy and power densities of high explosives to reach velocities greater than 10 km/s [3, 4].

A traditional issue with explosive launching is that direct explosive loading necessitates deliberate hydrodynamic deformation of the projectile. Decoupling the projectile from direct contact with the explosive and instead cumulating/focusing the detonation products or an intermediate gas onto the projectile can partially circumvent this limitation. Examples of this launching scheme include the UTIAS implosion driven launchers [5] and the Voitenko compressor [2, 6]. A key limitation encountered in these particular devices is that hemispherical focusing generates very high peak pressures for very short durations. This in turn necessitates that the launch cycle has to be operated far below

* Corresponding author. Tel.: +1-514-569-3606; fax:+1-514-398-7365.
*E-mail address:* jason.loiseau@mail.mcgill.ca.


doi:10.1016/j.proeng.2013.05.011

theoretical limits of focusing to prevent projectile destruction. Ultimately, this restricts projectile "soft-launch" capability to well below desired performance.

A more attractive option for explosive "soft-launching" is to use sequential radial implosion in a cylindrical geometry to in-turn drive a more gradual linear cumulation of high pressure driving gas. An example of this scheme is the Titov launcher, which uses a cumulative jet of detonation products from a hollow cylinder of explosive to aerodynamically drag a projectile up to hypervelocity [7-9]. This design is essentially limited only by the ability of the jet to outdistance the detonation wave and the ratio of projectile drag to projectile mass.

A similar cumulative linear implosion can be used to compress a light driver gas to very high enthalpy for the purpose of pumping a conventional gas gun. A unique mode of operation is also possible for this device where explosives are continued along the entire length of the launcher in order to implode the launch tube in a programmed fashion behind the projectile to maintain a high base pressure. Using detonation wave-shaping techniques, this programmed linear implosion can be used to gradually accelerate the projectile to velocities faster than the detonation velocity of the explosive. This type of implosion driven launcher was pioneered by the Physics International Company (PI) in the late 1960's [10-15]. Their final implementation was capable of launching a 2 g projectile up to 12.2 km/s using an accelerating explosive lens to implode the launch tube. Despite the impressive capabilities of this device, further development ceased before the limits of performance were fully explored. The purpose of the present study is to redevelop this launcher capability and this paper reviews the most recent developments and provides an overview of launcher design considerations.

## 2. Detailed description of device operation

The single-stage linear-implosion-driven hypervelocity launcher is analogous to a two-stage light gas where the piston-operated pump tube has been replaced by an explosive shock tube. The explosive shock tube consists of a pressurized thin-walled metal tube surrounded by an annulus of explosives which is in turn surrounded by a thick-walled metal casing. As with two stage light gas guns, the preferred fill gas is helium. The explosive layer is initiated at one end and a detonation wave travels along the length of the gas tube. This causes a sequential radial collapse of the tube, which in turn forms a pinch that travels at the detonation velocity of the explosive. The pinch acts like a piston and serves to drive a strong precursor shock wave (*PSW*) into the gas ahead of it. Since the shock travels up to 30% faster than the detonation wave, a column of high pressure gas is accumulated in the metal tube. This shocked gas can then be expanded against a projectile within a massive steel reservoir. In order to dynamically contain the high pressure driving gas as the projectile accelerates, additional explosives can be used to seal a conical section of the reservoir. A schematic of a single stage launcher in operation is depicted in Fig.. 1.

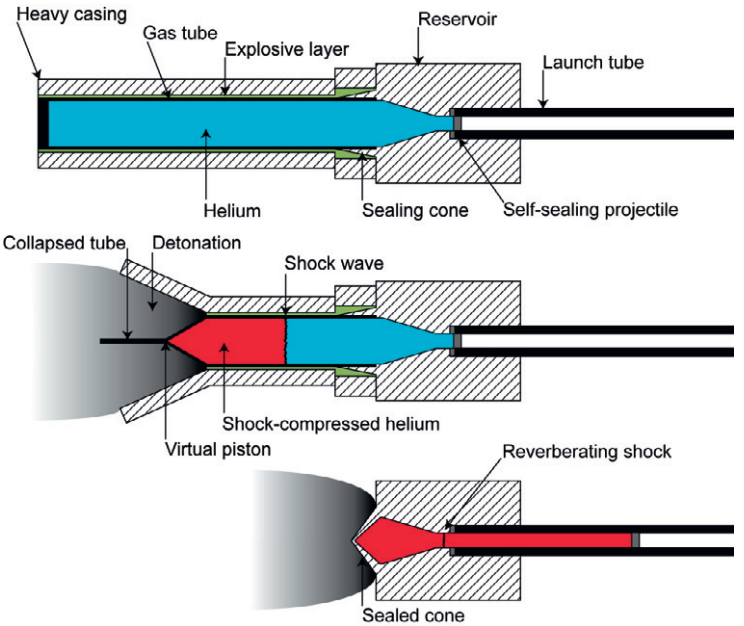


Fig.. 1. Schematic of a linear implosion driven hypervelocity launcher, showing stages of explosive operation.

## 3. Explosive shock tube properties

As an independent device, the explosive shock tube can be tuned to yield a wide range of post-shock states by varying the detonation velocity of the explosive and the initial fill pressure of the gas tube [16]. In the highly idealized case where the explosive pinch acts like a perfect piston, the tube walls are rigid until implosion and the driver gas behaves ideally, the *PSW* Mach number ($M_s$) can be described by the following equation, where $U_P$ is the velocity of the pinch, $c_0$ is the initial sound speed in the gas, and $\gamma$ is the ratio of the specific heats of the gas:

$$\frac{U_P}{c_0} = \frac{2}{\gamma + 1}\left(\frac{M_s^2 - 1}{M_s}\right)$$

Typical detonation velocities of readily available high explosives range from 4 km/s to 8 km/s, resulting in helium *PSW* velocities between 5.5 km/s and 11 km/s. In theory, because the *PSW* is continuously moving away from the pinch, an arbitrary long column of shocked gas could be accumulated and this would allow the launcher to operate as an infinite propellant-to-projectile mass ratio (*G/M*) light gas gun. In practice, a set of non ideal effects during explosive shock tube operation prevent the creation of extremely long gas columns.

As the pump tube is initially imploded, a diffuse metal jet is formed by the pinch [10]. Since this jet can travel significantly faster than the detonation wave (up to twice detonation velocity), it is believed to be responsible for the overdriven *PSW* velocity initially observed in experiments. Behind the *PSW*, pressures typically exceed the yield strength of most metals. For a shock velocity of 11 km/s, the pressure ratio is 150, resulting in post shock pressures approaching or exceeding 1 GPa for typical initial pressures (2-10 MPa/20-100 atm) of interest to launcher design. This dynamic pressurization causes the gas tube walls to expand behind the shock, which in turn attenuates *PSW* velocity. For higher initial fill pressures, if the *PSW* is sufficiently ahead of the explosive pinch, there may be sufficient time for the gas tube walls to expand until bursting. The resulting gas loss can significantly impair shock tube performance. Finally, as the *PSW* moves down the gas tube, a boundary layer grows along the tube walls behind it. Once the boundary layer reaches some critical thickness, a portion of the stagnant gas cannot be turned forward by the pinch and it is lost into the trailing slug of the collapsed gas tube. This leakage further attenuates the *PSW* until a quasi steady-state condition is reached where the shock moves at the velocity of the pinch, with a fixed standoff. The evolution of the *PSW* trajectory and the relative influence of the various non-ideal effects can be seen in Fig. 2, which plots the decay in shock velocity as a function of position for a long explosive shock tube experiment performed by Szirti [17]. Overlaid on the *v-x* plot are schematics that show the evolution of non-ideal effects and their zones of influence on *PSW* velocity.

The evolution of these non-ideal effects dictates the design of explosive shock tubes used to drive the hypervelocity launcher. The length to diameter ratio of the tube must be kept sufficiently small such that boundary layer losses do not reduce the enthalpy of the propellant gas delivered to the reservoir, which is essentially a function of the *PSW* velocity. In practice this restricts shock tube length to no more than 50 diameters. Furthermore, the gas tube, explosive layer, and outer

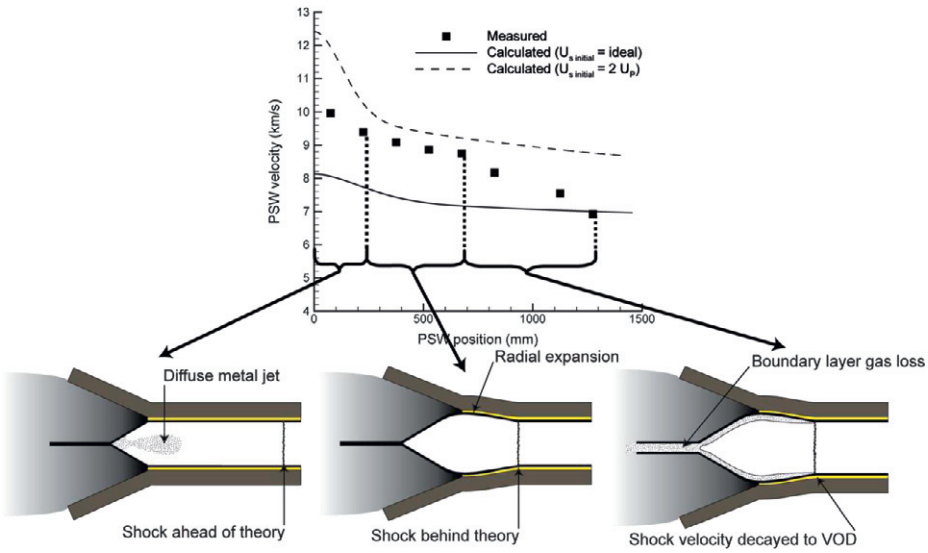


Fig. 2. Evolution of PSW velocity as a function of position for an experiment conducted by Szirti. The gas tube had an outer diameter of 12.7 mm and an inner diameter of 10.9 mm. Overlaid are schematics of the three main non-ideal effects influencing shock behaviour. Their regime of influence as a function of position are also identified.

casing must be designed in order to minimize expansion losses and prevent bursting. PI and Szirti identified that this can be accomplished by using a thin-walled gas tube clad with a thin explosive layer that is, in turn, confined by a thick-walled steel casing [12, 17]. This design scheme tampers the explosive layer thereby increasing the velocity and efficiency of the gas tube implosion, while the thin explosive layer facilitates rapid acoustic communication between the gas tube wall and the inner surface of the casing. The short acoustic travel time allows for compression waves reflected by the casing to dynamically confine the gas tube, thereby mitigating radial expansion and bursting. Iterative analytical models have been developed by Szirti and PI to predict the evolution of *PSW* attenuation from radial expansion and boundary layer leakage [10, 17]. Fig. 2 also illustrates the computed influence of radial expansion on *PSW* velocity for simulations where the velocity has been initialized at either twice the detonation velocity due to overdriving from the metal jet or at the theoretical velocity determined from Equation 1. By reducing the virtual piston velocity partway down the tube length it is also possible to reproduce a rarefaction fan that mimicks the attenuating effect of boundary layer gas loss. Unfortunately, due to uncertainties in initial *PSW* overdriving and the onset of boundary layer loss, these models are descriptive and not predictive.

## 4. Quantitative description of the launch cycle and launcher parameters

Shock compression of the helium results in a higher propellant pressure and temperature over shorter pump tube travel length compared to a two-stage light gas gun, allowing for the development of a relatively compact launcher. Since the linear implosion launcher is analogous to a two-stage light gas gun, its internal ballistic performance is dictated by many of the design parameters outlined in Seigel's seminal monograph, namely *G/M*, reservoir chambrage and launch tube length [18]. However the resulting extreme propellant state also leads to several unique design considerations which heavily influence the relative importance of these parameters.

Since the shock tube can dynamically operate at pressures well beyond the yield strength of most materials, the initial pump tube pressure must be adjusted, not for optimal theoretical performance, but to prevent destructive projectile loading. The extreme pressure also causes severe internal expansion of the reservoir; a phenomena that has been identified as the primary limiter of single stage launcher performance and one that significantly reduces the ability to increase launcher performance by increasing initial fill pressure.

A quasi-one-dimensional hydrocode with area change has been developed in order to simulate the launch cycle of the implosion launcher as well as determine the influence of a variety of design parameters. The numerical scheme is based on a code developed by the United States Naval Ordnance Laboratory and uses a VonNeumann and Richtmyer artificial viscosity shock capturing technique evolved by Noh [19, 20]. This hydrocode can also model the influence of domain boundary expansion or contraction due to internal pressurization or implosion via a series of 1-D radial hydrocode “slices” coupled to the internal ballistics hydrocode.

### *4.1. Idealized versus actualized launch cycle*

Using this hydrocode, an ideal launch cycle has been computed for two launcher sizes of interest: a 10 mm bore and a 25.4 mm bore launcher. The 10 mm launcher employs a 25 mm outer diameter gas tube that is 55 cm long ($L/D = 22$) and filled to a pressure of 34.5 atm with helium. The sealing cone is 38 mm long and the reservoir had a 12° conical transition from the gas tube inner diameter to the launch tube inner diameter. The 25.4 mm launcher employs a 76 mm outer diameter

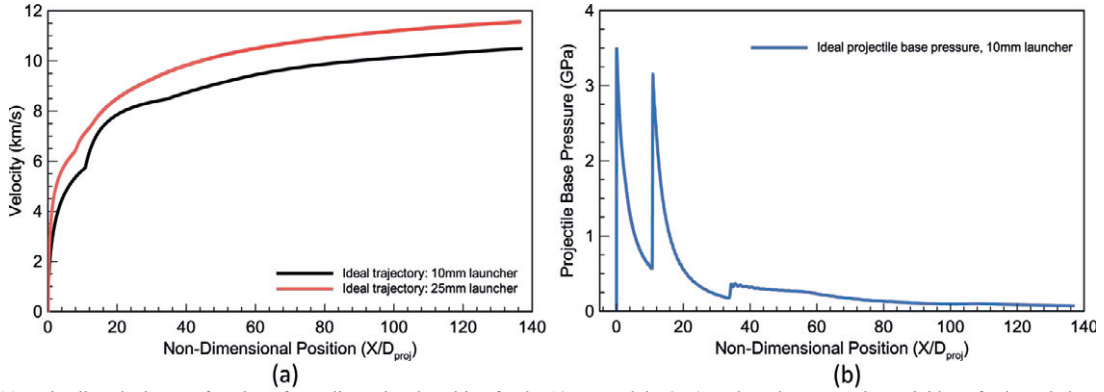


Fig. 3. (a) Projectile velocity as a function of non-dimensional position for the 10 mm and the 25.4mm launchers assuming a rigid, perfectly sealed launcher at fill pressures of 34.5 atm and 20 atm respectively. (b) Projectile base pressure as a function of non-dimensional position for the perfectly rigid and sealed 10mm launcher.

gas tube that is 183 cm long ($L/D$ = 24) and filled to 20 atm with helium. The sealing cone is 12 cm long and the reservoir has an 11.4° conical transition from the gas tube inner diameter to the launch tube inner diameter. The 10 mm launcher fires a 0.5 caliber long ZK60 projectile (mass of 0.72 g), while the 25.4 mm launcher fires a 0.5 caliber long ZK60 projectile massing 11.8 g. Calculations assume that the propellant is an ideal gas and that the explosive shock tube operates ideally owing to the relatively short length. The sealing cone is assumed to seal perfectly and the reservoir and launch tube are held rigid. The resulting projectile velocity and driving pressure histories are depicted in Fig. 3. Simulation results indicate that the 25.4 mm launcher can theoretically achieve projectile velocities around 12 km/s while the 10 mm launcher can achieve velocities of about 10 km/s for these fill pressures. Peak projectile base pressures of around 4 GPa are reached for both launch cycles. These peaks coincide with the arrivals of the initial *PSW* at the base of the project and subsequent re-reflections of the *PSW* by the sealing cone. The influence of launcher geometry on launcher internal ballistics will be discussed in subsequent sections.

In practice these ideal muzzle velocities cannot be reached due a set of non-ideal effects dominated by severe radial expansion of the reservoir section. Secondary non-ideal effects include *PSW* attenuation in the pump tube, gas leakage from the sealing cone and real gas effects. The relative influence of each of these non-ideal effects is shown in Fig. 4, where a series of hydrocode simulations of the 10 mm launcher at an initial fill pressure of 54 atm (5.5 MPa) were run with new ideal effects added in each simulation. While the idealized launch cycle predicts a muzzle velocity of nearly 12 km/s at this fill pressure, radial expansion alone reduces the predicted muzzle velocity to around 8 km/s. Conceptually, failure of the cone to seal should have a significant effect on muzzle velocity, however the influence of sealing failure is felt late in the launch cycle when a third re-reflected shock reaches the projectile, as indicated in Fig. 4(a). By this time, radial expansion of the reservoir has already significantly rarefied the propellant and the observed deficit in velocity from leaking is less than 100 m/s. However, if the launcher is held rigid, a deficit of nearly 2 km/s can be attributed to gas leakage and launcher performance is governed by the ratio of un-burst reservoir length to launch tube length ($x_0/x$) as defined in Fig. 5 [12]. Consequently the sealing cone remains a relevant design feature if explosives are used to dynamically confine the reservoir and thereby return the launcher to a more ideal level of performance.

Non-ideal pump tube behavior is modeled by correcting *PSW* stand-off and velocity with experimental data from Szirti [17]. Real gas behavior is modeled by using the Los Alamos SESAME equation of state database values for helium. As the pump tube is relatively short, it operates close to an ideal explosive shock tube, and thus *PSW* attenuation does not significantly reduce muzzle velocity. Likewise, the helium propellant does not depart from ideal gas behavior sufficiently to have a large effect on launcher performance. These two effects combine to reduce the muzzle velocity by another 200 m/s resulting a predicted velocity of 7.9 km/s, which is good agreement with the experimental result of 7.3 km/s.

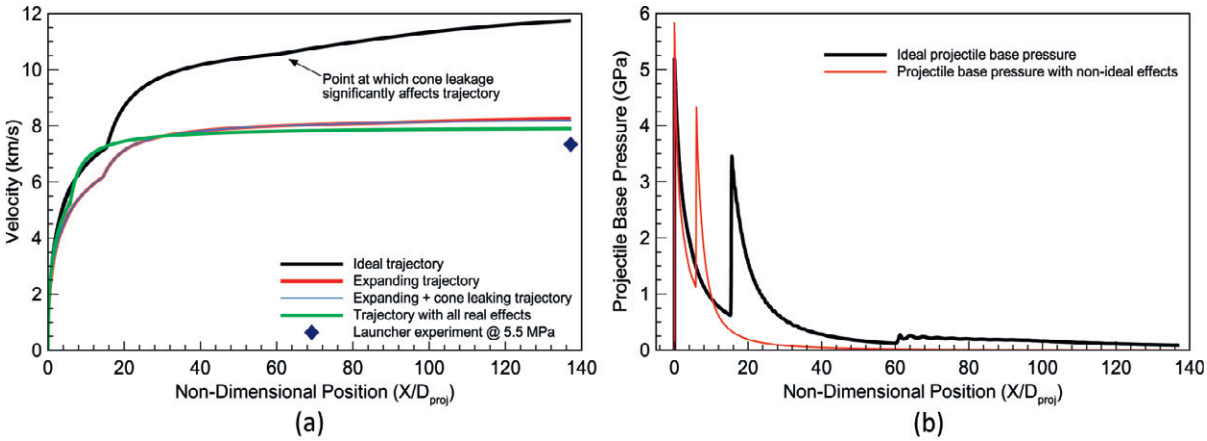


Fig. 4. (a) Projectile velocity as a function of non-dimensional position for the 10 mm launcher with an initial fill pressure of 54 atm. Individual curves show the influence of non-ideal effects on launcher muzzle velocity. (b) Projectile base pressure during ideal launch cycle compared to launch cycle including all non-ideal effects.

### *4.2. Influence of compression ratio and pump tube length*

The compression ratio (*CR*) of the launcher significantly influences the evolution of projectile back-pressure and shock behavior within the reservoir. This parameter is defined as the distance from the start of the pump tube to the projectile base divided by the final length of the reservoir after implosion of the sealing cone, as shown in Fig. 5. This parameter is thus

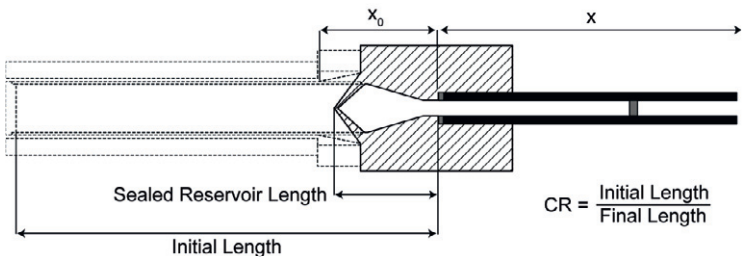


Fig. 5. Definition of compression ratio.

governed by the length of the pump tube and the length of the reservoir. The compression ratio can be seen as a shock timing parameter as it controls the duration required for the initial incident shock entering the reservoir to reflect off the projectile and return back to the reservoir inlet. Optimally, the reservoir length should be tailored relative to the gas tube length such that the detonation wave implodes the sealing cone as the reflected shock returns to the reservoir inlet plane. Ideally, this ensures that a strong shock is re-reflected towards the projectile early in the launch cycle, thereby increasing projectile acceleration. If the reservoir is made too long, a rarefaction fan emanating from the stopped explosive pinch will reduce reservoir pressure and thus ballistic performance. Additionally, the re-reflected shock will not be able to significantly contribute to enhancing projectile velocity. If the reservoir is made too short, the reflected shock can re-emerge into the gas tube before the sealing cone has a chance to close the reservoir, causing rupturing and propellant gas loss.

Experiments conducted by Tanguay examined the influence of compression ratio on terminal velocity for launchers with large projectile length to diameter (*L/D)* ratios [21]. While projectile terminal velocity was relatively insensitive to *CR*, it was observed that velocity increased with increasing *CR* until the point where the time of arrival of the reflected shock at the reservoir was coincident with the implosion of the sealing cone. Beyond this ratio, terminal velocity began to decrease with increasing compression ratio. This experimental series confirmed that the optimal compression ratio occurs when the reservoir is just short enough to ensure prompt re-reflection from the sealing cone but no shorter. For typical launcher gas tube lengths of around 50 diameters the value of *CR* should thus be maintained around 9.

Since *CR* is essentially determined by selecting an appropriate reservoir length based on the pump tube length, the influence of this latter parameter on launcher performance is a critical factor in launcher design. Pump tube length determines the quantity of gas delivered to the reservoir and thus launcher *G/M*, however *PSW* attenuation due to boundary layer formation and radial expansion limits the actual *G/M* and reduces propellant enthalpy. The influence of this behavior on launcher muzzle velocity is best described through simulation. A series of hydrocode calculations of the 10 mm launcher were performed that varied pump tube *L/D* from 20 to 60 with *PSW* trajectory adjustments based on experimental data [17]. Resulting muzzle velocity calculations are plotted against pump tube *L/D* in Fig. 6(a). According to these simulations, launcher muzzle velocity plateaus for an *L/D* of around 40, while diminishing returns can be obtained up to non-dimensional lengths of 60. From a design perspective the pump tube should be kept around 40 diameters long to most efficiently use availlable explosives. This value also closely coincides with the non-dimensional length of 50 diameters where significant losses in PSW velocity are observed.

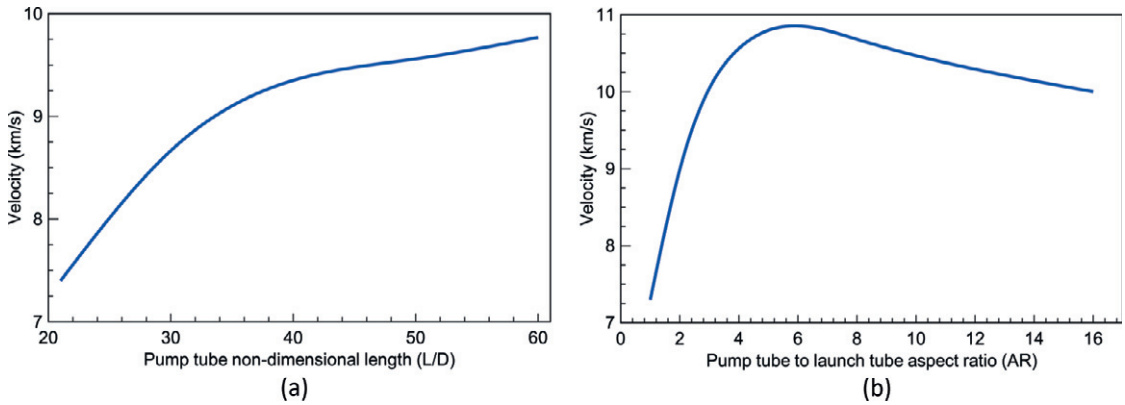


Fig. 6. (a) Computed launcher muzzle velocity versus pump tube non-dimensional length illustrating diminishing returns in launcher performance from elongating the pump tube. (b) Computed muzzle velocity versus launcher area ratio illustrating optimal launcher chambrage.

### 4.3. Influence of area ratio

As with a light gas gun, performance of the linear implosion gun is also influence by chambrage between the reservoir and the launch tube. However, due to the shock dynamics in the reservoir, performance gains from increasing chambrage cannot be actualized in a similar manner due to shock dynamics within the reservoir. As the *PSW* travels through a reservoir constriction it magnifies in intensity. Consequently, a launcher with a larger area ratio (*AR*) between the gas tube and launch tube will produce a larger peak loading on the projectile for a given initial fill pressure. Since peak loading influences projectile failure, a larger *AR* necessitates operating the launcher at a lower initial fill pressure in order to preserve a given loading condition. This requirement hampers the *G/M* advantage that could otherwise be obtained with increased launcher *AR*. A series of hydrocode simulations were conducted to investigate terminal ballistic gains that can be made by increasing launcher *AR* without scaling *CR* using the 10 mm launcher template. Initial fill pressure was scaled so that the peak launch cycle pressure was maintained at 5 GPa. These results are depicted in Fig. 6(b) and show that significant gains of about 3 km/s are realized by transitioning from a constant area launcher to a chambered launcher with an area ratio of about 5. After this point, performance slowly drops as *AR* is increased. These results indicated that further velocity gains cannot be obtained by transitioning to an effectively infinite *G/M* launcher by simply increasing the *AR*.

### 4.4. Influence of projectile areal density

Launcher performance can be directly linked to the areal density of the projectile due to the early onset of reservoir expansion. Hydrodynamic expansion of the reservoir is estimated to occur very early in the launch cycle, causing an immediate deviation from ideal internal ballistics calculations. This effect can be partially mitigated simply by minimizing the mass of the projectile for a given launcher bore in order to maximize projectile acceleration early in the launch cycle, where pressure remains relatively un-attenuated.

The importance of using a projectile with a low areal density can be observed by comparing a series of hydrocode simulations of the 10 mm launcher where successive simulations increase the length, and thus mass of the projectile. In these simulations, the reservoir is allowed to expand under the influence of internal pressure and an efficiency is computed by comparing the resulting muzzle velocity to the simulated case where the reservoir geometry remains rigid. Results are plotted in Fig. 7 and indicate that significant losses are incurred as projectile areal density is increased. The low areal density requirement entails reducing projectile thickness to the minimum required to retain in-bore stability and using low density materials despite the attendant strength penalties.

## 5. Experimental results

Two experimental campaigns were conducted using the 10 mm and 25 mm launcher geometries described in Section 4.1. These experiments were designed to optimize projectile design, verify launcher scalability and ultimately determine the practical limit on muzzle velocity for single-stage linear implosion driven launchers.

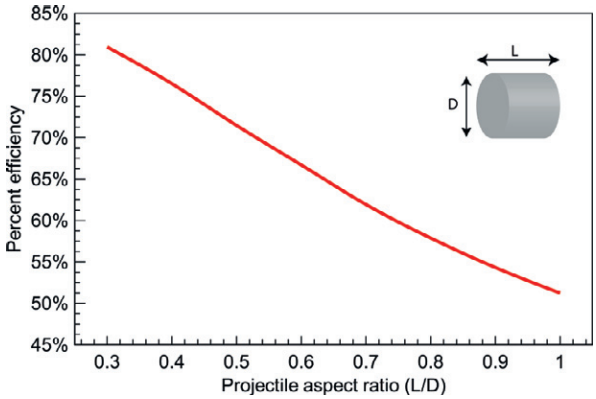


Fig. 7. Launcher efficiency as a function of projectile L/D.

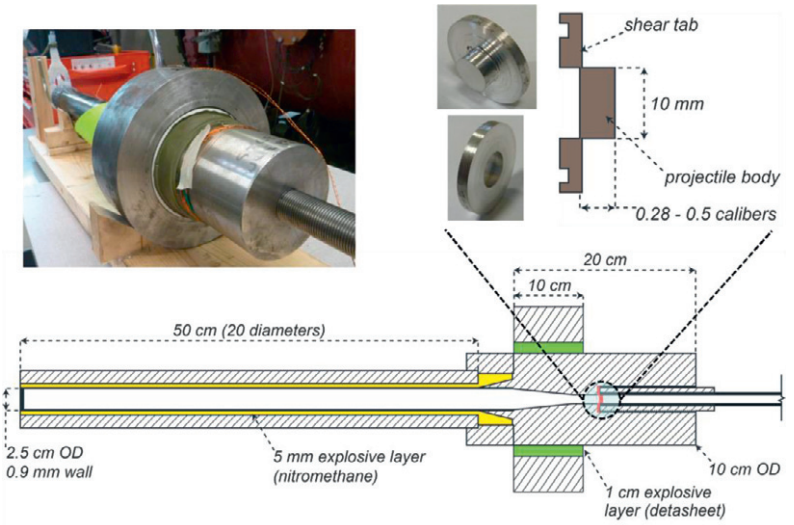


Fig. 8. Schematic and images of 10 mm launcher design details.

### *5.1. 10 mm launcher experiments*

The base geometry of the 10 mm launcher is described in Section 4.1 and a scale drawing of the design is depicted in Fig. 8. The gas tube wall thickness was 0.9 mm and a 5 mm layer of sensitized nitromethane (10% diethyltriamine by weight, detonation velocity of 6.0 km/s) was used to drive the tube implosion. The gas tube casing wall was 14 mm thick. The reservoir was 20 cm long and had a diameter of 10 cm. The launch tube was 180 cm long. All launcher components were made of mild steel except the launch tube, which was 4130 steel. In a subset of experiments, an annulus of detasheet (detonation velocity of 7 km/s) and a heavy steel ring were added around the conical area change section to partially counteract the effect of reservoir expansion. This secondary charge is also depicted in Fig. 8.

The projectile used a single piece, self-sealing design. The cylindrical projectile main-body was held within a support ring by a thin web of material typically 0.25 mm thick that was sufficiently strong to hold the initial gas tube pressure. Once the projectile is struck by the incident shock, the web shears and the projectile is set in motion. A sketch and images of a ZK60 projectile can also be seen in Fig. 8. Projectile length varied from 0.28 calibers to 0.5 calibers depending on the experiment. In addition to the ZK60 magnesium, aluminum 7075 and Ultem 1000 were used in certain experiments.

A series of six experiments were conducted in order to optimize the projectile configuration and determine the limits on initial fill pressure. The flight of each projectile was filmed with a Photon SA5 high-speed camera, allowing for the determination of velocity, integrity, and orientation. A witness plate was also used to determine projectile integrity. A summary of all six experiments is included in Table 1.

| Launcher | Projectile | Mass | Fill Pressure | Velocity |
|---|---|---|---|---|
| 10mm - 01 | 0.28 L/D, Al 7075 | 0.62 g | 34 atm | 7.89 km/s |
| 10mm - 02 | 0.28 L/D, Al 7075 | 0.62 g | 44 atm | 7.12 km/s |
| 10mm - 03 | 0.35 L/D, Mg ZK60 | 0.50 g | 34 atm | 7.36 km/s |
| 10mm - 04 | 0.50 L/D, Mg ZK60 | 0.72 g | 54 atm | 7.34 km/s |
| 10mm - 05 | 0.50 L/D, Mg ZK60 | 0.72 g | 68 atm | 7.46 km/s |
| 10mm - 06 | 0.50 L/D, Ultem | 0.50 g | 34 atm | 7.24 km/s |

Table 1. Summary of 10 mm launcher results including projectile properties, masses and initial fill pressures.

The two initial experiments employed 0.28-caliber-long aluminum 7075 projectiles to minimize weight and areal density. The first experiment used an initial helium fill pressure of 34 atm and the projectile was launched intact to a velocity of 7.89 km/s. A series of frames of the projectile in flight can be seen in Figure 9, which shows the projectile moving from right to left with a slight cant and a luminescent muzzle jet attached to the base. The reservoir section was observed to have

expanded without rupture and the sealing cone imploded properly. In the second experiment, the fill pressure was increased to 44 atm. Once again the reservoir did not rupture and the cone sealed properly, however the projectile velocity was only 7.12 km/s and the projectile was tumbling significantly in flight, as can be seen in Fig. 10. In a similar experiment, where the projectile was replaced with a lighter, 0.35-caliber-long ZK60 projectile and the launcher was operated at an initial fill pressure of 34 atm, the projectile was once again tumbling and reached a velocity of only 7.36 km/s. Since lowering the mass or increasing the fill pressure is expected to increase muzzle velocity, the losses observed in these two experiments was attributed to projectile tumbling and propellant blow-by.

In all subsequent experiments the projectile length was increased to 0.50 calibers. In order to compensate for the increase in mass in the ZK60 projectiles, the initial fill pressure was also increased to 54 atm and then to 68 atm. The shot at 54 atm resulted in a projectile velocity of 7.34 km/s with partial fracturing of the reservoir and a sealed cone. The shot at 68 atm produced a velocity of 7.46 km/s while the reservoir fractured completely and the cone was destroyed. Both projectiles were flying straight without tumbling. These experiments highlight that significant gains in velocity cannot be made by simply increasing initial fill pressure because of the increase in reservoir expansion and failure related losses.

The final experiment attempted to reduce projectile mass/areal density and return to a lower operating pressure by switching to an Ultem 1000 plastic projectile. Initial fill pressure was 34 atm, and the reservoir and sealing cone remained intact. The projectile velocity was only 7.24 km/s and the high speed movie revealed that the projectile was launched intact but severely ablated. The relatively low velocity is attributed to ablation and propellant blow-by, which suggests that alloys are a superior projectile material for this application despite the higher density.

In an effort to reduce losses due to radial expansion, the subsequent experiment added the 1-cm-thick annulus of detasheet to partially implode the reservoir. The initial fill pressure was reduced to 54 atm and the projectile was launched intact to 7.92 km/s. The projectile in flight can be seen in Fig. 11. The secondary annulus was initiated sequentially 75 μs after the main charge was initiated. This was done to prevent stress waves generated by the detonation of the annulus from reaching and potentially damage the projectile. In comparison to previous results, the addition of dynamic explosive confinement increased muzzle velocity by about 500 m/s. Losses to reservoir radial expansion were still significant, however. This can be seen in Fig. 12, which depicts a photograph of a reservoir sectioned in half post-experiment.

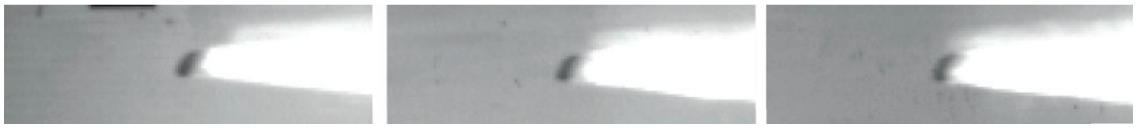

Fig. 9. Frames of a 0.28-calibre-long Al 7075 projectile travelling from right to left at 7.89 km/s with attached muzzle jet.

Fig. 10. Frames of a tumbling 0.28 calibre long Al 7075 projectile travelling from right to left at 7.12 km/s.

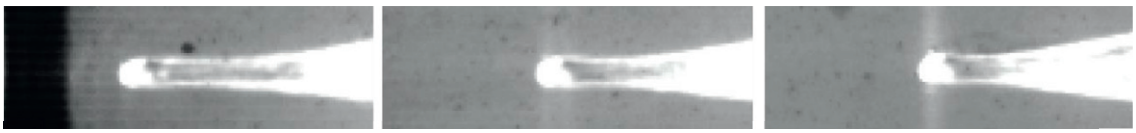

Fig. 11. Frames of a 0.50 calibre long ZK60 projectile in flight at 7.92 km/s. Muzzle jet is still attached to projectile.

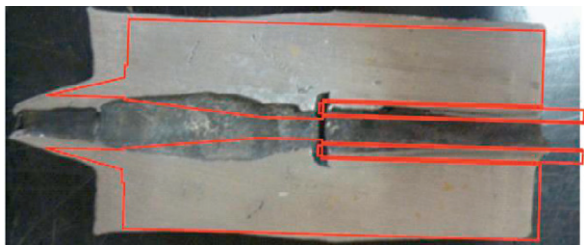

Fig. 12. Sectioned reservoir showing internal expansion and partial implosion of the outer surface. Red overlay shows original dimensions.

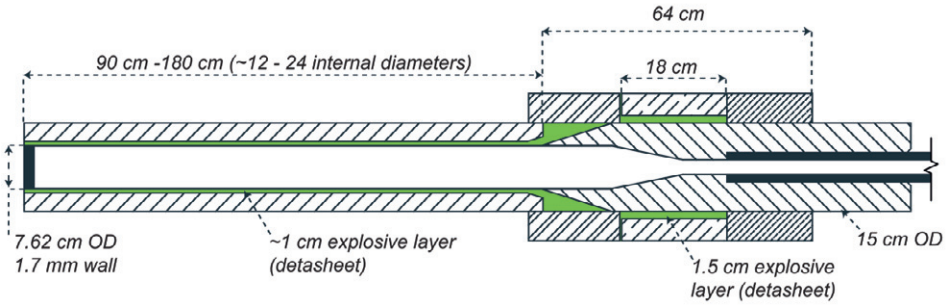


Fig. 13. Scale Schematic of 25mm bore launcher

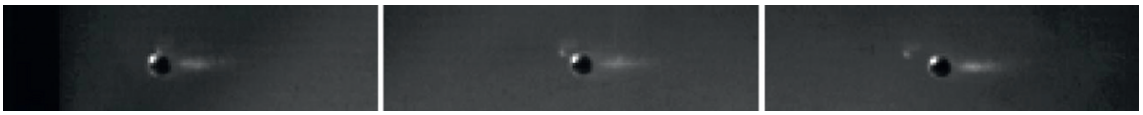

Fig. 14. 25mm diameter (0.5 calibre long) Al 7075 projectile in flight at 7.55 km/s.

### *5.2. 25 mm large scale launcher experiment*

A large scale experiment was conducted based on the 25 mm launcher template discussed in Section 4.1. The gas tube wall thickness was 1.7 mm and it was surrounded by 6 mm of detasheet. The gas tube casing had a wall thickness of 32 mm. The reservoir was 51.5 cm long and had an outer diameter of 15 cm. A 13-mm-thick layer of detasheet surrounded by a 38-mm-thick steel ring was used to dynamically confine the reservoir against expansion. This explosive layer was also timed such that the resulting stress wave would not be able to interact with the projectile. The launch tube was 182 cm long. A schematic of the launcher is depicted in Figure 13.

The projectile was 0.5 calibers long and was made from Al 7075 and used a conventional diaphragm rather than the self-sealing design. Projectile mass was 15 g. At a fill pressure of 20 atm the projectile was launched intact to 7.55 km/s. Frames of the movie are depicted in Fig. 14.

## 6. Conclusion

Even with partial explosive confinement, the single stage devices discussed in Section 5 have approached the maximum muzzle velocity believed possible due to radial expansion of the reservoir. These results are closely matched by hydrocode simulations that model the influence of reservoir expansion and several other non-ideal effects. Despite the limitation on muzzle velocity, the device displayed excellent scalability in projectile mass/launcher bore size without appreciable loss in maximum velocity.

In order to actualize higher velocities, complete implosion of the reservoir must be achieved using thicker layers of explosive and implosion must be continued along the entire launch tube in a programmed fashion. A explosive shock tube based around an asymmetric implosion scheme is anticipated to provide the required launch tube implosion [22, 23]. Implementation of these additional launcher stages is expected to be able to increase projectile velocity beyond 10 km/s.

## References

[1] L.A. Glenn, On How to Make the Fastest Gun in the West, in: International Workshop on New Models and Numerical Codes, St. Catherine's College, Oxford, UK, 1997.
[2] L.A. Glenn, Design Limitations on Ultra-High Velocity Projectile Launchers, Int. J. Impact Eng., 10 (1990) 185-196.
[3] A.B. Wenzel, A review of explosive accelerators for hypervelocity impact, Int. J. Impact Eng., 5 (1987) 681-692.
[4] A.J. Higgins, J. Loiseau, J. Huneault, The Application of Energetic Materials to Hypervelocity Launchers, International Journal of Energetic Materials and Chemical Propulsion, (2012).
[5] I.I. Glass, Appraisal of UTIAS implosion-driven hypervelocity launchers and shock tubes, Progress in Aerospace Sciences, 13 (1972) 223-291.
[6] A. Voitenko, V. Kirko, Efficiency of a high-explosive plasma compressor, Combustion, Explosion, and Shock Waves, 11 (1975) 813-815.
[7] I.A. Stadnichenko, V.M. Titov, V.P. Chistyakov, G.A. Shvetsov, Investigations and certain applications of explosive shock tubes, Combustion,

Explosion, and Shock Waves, 18 (1982) 335-341.
[8] L.A. Merzhievskii, V.M. Titov, Y.I. Fadeenko, G.A. Shvetsov, High-speed launching of solid bodies, Combustion, Explosion, and Shock Waves, 23 (1987) 576-589.
[9] P.A. Lazorskii, A.V. Plastinin, V.V. Sil'vestrov, V.M. Titov, Acceleration of solid particles during cumulation of detonation products in vacuum, Combust. Explos., 35 (1999) 443-446.
[10] E.T. Moore, Explosive Hypervelocity Launchers, NASA CR-982, Physics International Company, 1968
[11] J.D. Watson, A Summary of the Development of Large Explosive Guns for Reentry Simulation, PIFR-155, Physics International Company, 1970
[12] J.D. Watson, High-Velocity Explosively Driven Guns, NASA CR-1533, Physics International Company, 1970
[13] D.W. Baum, Development of Explosively Driven Launcher for Meteoroid Studies, NASA CR-2143, Physics International Company, 1973
[14] D.W. Baum, Explosively Driven Hypervelocity Launcher Second-Stage Augmentation Techniques, PIFR-245-1, Physics International Company, 1973
[15] K. Seifert, Feasibility Study of Explosively Driven Hypervelocity Projectiles, PIFR-559, Physics International Company, 1974
[16] V.B. Mintsev, V.E. Fortov, Explosion-driven shock tubes/Review, High Temperature, 20 (1982) 623-645.
[17] D. Szirti, J. Loiseau, A. Higgins, V. Tanguay, Dynamics of explosively imploded pressurized tubes, J Appl Phys, 109 (2011) 084526-084526-084516.
[18] A.E. Seigel, The Theory of High Speed Guns, AGARDograph, 1965.
[19] J. Vonneumann, R.D. Richtmyer, A Method for the Numerical Calculation of Hydrodynamic Shocks, J Appl Phys, 21 (1950) 232-243.
[20] W.F. Noh, Errors for calculations of strong shocks using an artificial viscosity and an artificial heat flux, Journal of Computational Physics, 72 (1987) 78-120.
[21] V. Tanguay, D. Szirti, J. Loiseau, A.J. Higgins, Development of a Hypervelocity Launcher Based on Implosion, in: Hypervelocity Impact Symposium, 2010.
[22] J. Loiseau, J. Huneault, M. Serge, A. Higgins, V. Tanguay, Phase velocity enhancement of linear explosive shock tubes, AIP Conference Proceedings, 1426 (2012) 493-496.
[23] J. Loiseau, D. Szirti, A.J. Higgins, V. Tanguay, Experimental technique for generating fast high-density shock waves with phased linear explosive shock tubes, Shock Waves, 22 (2012) 85-88.